A New Class of Nonlinear PID Controllers for Robotic Applications

Homayoun Seraji
Jet Propulsion Laboratory
California Institute of Technology
Pasadena, CA 91109, USA

Abstract

This paper introduces a new class of simple nonlinear PID-type controllers comprised of a sector-bounded nonlinear gain in cascade with a linear fixed-gain P, PD, PI, or PID controller. Three simple nonlinear gains are proposed: the sigmoidal function, the hyperbolic function, and the piecewise-linear function. The systems to be controlled are assumed to be modeled or approximated by second-order transfer-functions, which can represent many robotic applications. The stability of the closed-loop systems incorporating nonlinear P, PD, PI, and PID controllers are investigated using the Popov Stability Criterion. It is shown that for P and PD controllers, the nonlinear gain is unbounded for closed-loop stability. For PI and PID controllers, simple expressions are derived that relate the controller gains and system parameters to the maximum allowable nonlinear gain for stability. A numerical example is given for illustration.

1 Introduction

Undoubtedly, PID controllers have been the most popular and the most commonly used industrial controllers in the past fifty years. The popularity and widespread use of PID or three-term controllers is attributed primarily to their simplicity and performance characteristics, where the I term ensures robust steady-state tracking of step commands while the P and D terms provide stability and desirable transient behavior. PID controllers have been utilized for the control of diverse dynamical systems ranging from industrial processes to aircraft and ship dynamics. In fact, industrial robotic manipulators invariably use PID controllers in their independent joint servo control systems.

While linear fixed-gain PID controllers are often adequate for controlling a nominal physical process, the requirements for high-performance control with changes in operating conditions or environmental parameters are often beyond the capabilities of simple PID controllers.

For instance, when a robotic arm is, contacting a reaction surface with a known stiffness coefficient, a linear fixed-gain PID controller can be designed to achieve a desirable force response with zero steady-state error, low overshoot, and rapid rise time. However, the same controller typically exhibits a sluggish response in contact with softer surfaces, and becomes unstable when contacting harder surfaces. In other words, because the stiffness coefficients of different reaction surfaces can differ substantially, a fixed-gain PID controller design based on a nominal surface stiffness leads to a non-uniform dynamic performance and often instability. This problem can be alleviated, to a large extent, by employing nonlinear elements in the PID control scheme. These elements can compensate for stiffness variations and yield stable and uniform responses. Even when the reaction surface stiffness is constant and known, a nonlinear PID controller can result in superior command tracking and disturbance rejection performances compared to linear fixed-gain PID controllers, as demonstrated in a recent paper on a nonlinear PD controller for robot contact control [1].

This paper presents a simple enhancement to the conventional PID controller by incorporating a nonlinear gain in cascade with a linear fixed-gain PID controller. This enhancement enables the controller to *adapt* its response based on the performance of the closed-loop control system. When the error between the commanded and actual values of the controlled variable is large, the gain amplifies the error substantially to generate a large corrective action to drive the system output to its goal rapidly. As the error diminishes, the gain is automatically reduced to prevent large overshoots in the response. Because of this automatic gain adjustment, the nonlinear PID controller enjoys the advantage of high initial gain to obtain a fast response, followed by a low gain to prevent large overshoots.

The paper is structured as follows. The problem is stated in Section *2*. Absolute stability of the closed-loop systems incorporating nonlinear P, PD, PI, and PID controllers are investigated in Sections 3–6. A numerical example is given in Section 7 for illustartion. Finally, conclusions drawn from this work are presented in Section 8.

2 Problem Statement

In this section, we describe the system under control and discuss its performance using a nonlinear PID controller.

2.1 System Description

In many robotic applications, the dynamics of the system to be controlled can be adequately modeled by a second-order differential equation. Even when the system dynamics is of higher order, the response of the system is often largely dependent on the location of a pair of *dominant complex poles,* which can be embodied in a second-order model [2]. Examples of such robotic systems are: joint servo dynamics, arm Cartesian dynamics, force control, and compliance/impedance control. In these systems, the second-order transfer-function relating the system output $y(t)$ to the control input $u(t)$ is given by

$$G(s) = \frac{y(s)}{u(s)} = \frac{\omega_n^2 \hat{k}}{s^2 + 2\xi\omega_n s + \omega_n^2} = \frac{c}{s^2 + as + b} \quad (1)$$

where ξ, ω_n, and $\hat{k}$ denote, respectively, the damping ratio, natural frequency, and DC gain of the system, $a = 2\xi\omega_n$, $b = \omega_n^2$, and c = $\omega_n^2 \hat{k}$.

The new class of controllers presented in this paper consists of a nonlinear gain k in cascade with a linear fixed-gain PID-type controller K(s) = $k_p + \frac{k_i}{s} + k_d s$, where k_p, k_i, and k_d are the positive or zero constant proportional, integral, and derivative gains, respectively. The nonlinear gain k acts on the error $e(t) = y_r(t) - y(t)$ between the actual output $y(t)$ and the desired output y,(t), and produces the "scaled" error $f(t) = k(e)\ .e(t)$, where $k(e)$ denotes a function of e. The scaled error $f(t)$ is then inputted to the PID controller K(s) which generates the control action $u(s)$ = K(s) f(s) to drive the system, as shown in Figure la. Three choices for the nonlinear gain k are discussed next.

2.2 Nonlinear Gains

The gain k can represent *any* general nonlinear function which is bounded in the sector O < $k < k_{max}$. The input-output characteristics of the sector-bounded nonlinear gain k is depicted in Figure lb; showing that the output f lies within the shaded sector O < $f < k_{max}.e$. There is a broad range of options available for the nonlinear gain k. Here, we propose three examples of such functions. The first proposed nonlinear gain k *as* a function of the error e is the smooth *sigmoidal* function

$$k = k_o + k_1 \left\{ \frac{2}{1 + exp(-k_2 e)} - 1 \right\} \quad (2)$$

where k_o, k_1, and k_2 are user-defined positive constants. The gain k is lower-bounded by $k_{min} = k_o - k_1$ when e = –00, is upper-bounded by $k_{max} = k_o + k_1$ when e = $+\infty$, that is $k_{min} < k < k_{max}$, and furthermore $k = k_o$ when e = O. Thus k_o defines the *central value* of k, k_1 determines the *range of variation* of k(= $k_{max} - k_{min} = 2k_1$) with $k_1 \leq k_o$ to ensure $k > 0$, while k_2 specifies the *rate of variation* of k. Figure 2a shows a typical variation of k as a function of e when $k_o = 2$, $k_1 = 1$, and $k_2 = 0.5$, and shows that k has an 'S-shaped" curve. Notice that using equation (2), the nonlinear gain k has equal excursions of $\pm k_1$ for positive and negative error e. When unequal ± excursions of k are required, the error e in equation (2) is replaced by the shifted error e + A, where A is a user-specified constant. When A >0, the plot of k versus e from equation (2) is shifted to the left by the amount A, and the excursion of k for negative e is larger than that for positive e. Likewise, when A < 0, the plot is shifted to the right by A, and the excursion of k for positive e is larger than that for negative e. Thus, by a judicious choice of A, we can attain the desired unequal excursions of k for $\pm e$.

The second proposed choice for the gain k *as* a function of the error e is the *hyperbolic* function

$$k = k_o + k_1\left\{1 - \frac{2}{exp(k_2 e) + exp(-k_2 e)}\right\} \quad (3)$$

$$= k_o + k_1\{1 - sech(k_2 e)\} \quad (4)$$

where k_o, k_1, and k_2 are user-defined positive constants. The gain k is now upper-bounded by $k_{max} = k_o + k_1$ when $e = \pm\infty$, and lower-bounded by $k_{min} = k_o$ when e = O. Thus k_o defines the minimum *value,* k_1 denotes the *range of variation,* and k_2 specifies the *rate of variation* of *k.* Figure 2b shows a typical variation of k versus e when k_o=1, k_1=l, and k_2=0.5. It is seen that k is an "inverted bell-shaped" curve, and is an even function of e, that is $k(-e) = k(e)$. This class of nonlinear gains is applicable when k is required to be a function of the error magnitude $|e|$.

The third class of nonlinear gains that can be used are *piecewise-linear* functions. For example, k can be chosen as a bounded piecewise-linear function of e as

$$k = \begin{cases} k_{max} & \text{for e} \geq e_{max} \\ k_o + k_1 e & \text{for O} < \text{e} < e_{max} \\ k_o + k_2 e & \text{for } e_{min} < \text{e} < 0 \\ k_{min} & \text{for e} \leq e_{min} \end{cases} \quad (5)$$

where k. is the central value (for e = O), k_1 and k_2 are the slopes for $\pm e$, and (k_{max}, e_{max}) and (k_{min}, e_{min}) are the upper and lower bounds, respectively. A typical variation of k versus e is shown in Figure 2C for $k_{max} = 5, k_{min} = 1, k_o = 2, k_1 = 0.5, k_2 = 1, e_{max} = 6$, and $e_{min} = -1$. In the special case when $k_{min} = k_o = k_2 = 0$ and $e_{min} = 0$, we obtain $k = 0$ for $e \leq 0, k = k_1 e$ for O < e < e_{max}, and $k = k_{max}$ for e $\geq e_{max}$. This type of nonlinear gain is used in a robot collision avoidance control system [3].

2.3 System Performance

The motivation for using the nonlinear gain k is now discussed qualitatively. Consider the closed-loop control system shown in Figure la. When k is a constant, the linear PID controller gains can be chosen such that for a step command input, the closed-loop system exhibits either an oscillatory fast response with overshoot or a monotonic slow response with no overshoot. In other words, the linear PID controller is incapable of accomplishing the two contradictory requirements of a fast response and no overshoot simultaneously. On the other hand, when the gain k is a nonlinear function of the error e, such as the sigmoidal function defined earlier, initially the error e between the command y_r and the output y is large, hence the gain k will be large, producing a fast response. As time proceeds and the error e is diminished, the gain k will be reduced automatically. When the output y overshoots the command y_r, the gain k is reduced even further, thus inhibiting further overshoot. Therefore, the automatic adjustment of the gain k as a function of the error e can produce a fast response with a

small overshoot, a behavior that is unattainable by a linear fixed-gain PID controller. This argument can be repeated when the system is subjected to disturbance inputs, whereby the nonlinear gain enables the system to exhibit a fast non-oscillatory response.

For the sake of illustration, *Matlab* is used to simulate the control system shown in Figure la with the linear plant G(s) = $\frac{25}{s^2+20s+25}$, the fixed-gain PI controller K(s) = 5 + $\frac{5}{s}$, and the nonlinear gain k. For a constant gain of $k = 1$, the unit step response (at $t = 0.1$ *see)* of the closed-loop system is shown in Figure 3a, indicating that the transient response is slow with the settling time of about 0.5 sec. Now, let us use the nonlinear gain k as a hyperbolic function of the tracking-error e, that is, $k = 1 + 4\left[1 - \frac{2}{exp(e)+exp(-e)}\right]$, where k can now vary in the range $1 \leq k \leq 5$ depending on the value of e. The closed-loop unit step response is shown in Figure 3b, exhibiting a fast transient response with the settling time of 0.2 sec and no overshoot. By comparing Figures 3a and 3b, it is clear that the nonlinear gain has improved the system response considerably by speeding up the transient response without causing oscillations. The variation of the gain k versus time is shown in Figure 3c, exhibiting a sudden rise from the initial value $k(0) = 1$ to about 2.4 and then drop back to 1 after 0.2 sec when the steady-state is reached. This transient change in k is responsible for the reduction in the settling time without ensuing oscillations, and hence the improvement in the step response. Note that obtaining such a fast response using a linear PI controller yields an oscillatory behavior.

Consider now the closed-loop control system shown in Figure la with a *general* sector-bounded nonlinear gain k depicted in Figure lb. Because of the nonlinear nature of k, the stability analysis of the closed-loop system is non-trivial. We shall now present the stability analysis of the closed-loop systems with different types of nonlinear PID controllers.

3 Stability Analysis of Nonlinear P Controllers

In this case, the closed-loop system employs the proportional (P) controller

$$K(s) = k_p \tag{6}$$

in cascade with the nonlinear gain k, where k_p is the positive constant proportional gain.

To investigate the absolute stability of the closed-loop system, we combine the linear components (1) and (6) as

$$\text{W(s)} = G(s)K(s) = \frac{ck_p}{s^2 + as + b} \tag{7}$$

which is a second-order transfer-function, and separate out the nonlinear element which is the gain k. We can now apply the Popov Stability Criterion [4, 5] to the system by examining the Popov plot of $W(j\omega)$, which is the plot of $\mathcal{R}eW(j\omega)$ versus $\omega\mathcal{I}mW(j\omega)$, with ω as a parameter and $\mathcal{R}e$ and $\mathcal{I}m$ refer to the real and imaginary parts, respectively. This plot

reveals the range of values that the nonlinear gain k can assume while retaining closed-loop stability. The Popov Criterion can be stated graphically as follows:

"A *sufficient* condition for the closed-loop system to be absolutely stable for all nonlinear gains in the sector O < k < k_{max} is that the Popov plot of W $(j\omega)$ lies entirely to the right of a straight-line with a non-negative slope passing through the point $-\frac{1}{k_{max}} + j0$."

In order to apply the Popov Criterion to the system, we need to compute the crossing of the Popov plot of $W(j\omega)$ with the real axis. In this case, from equation (7), we obtain

$$\mathcal{R}eW(j\omega) = \frac{ck_p(b-\omega^2)}{a^2\omega^2+(b-\omega^2)^2} \tag{8}$$

$$\omega\mathcal{I}mW(j\omega) = \frac{-ack_p\omega^2}{a^2\omega^2+(b-\omega^2)^2} \tag{9}$$

Thus the Popov plot of $W(j\omega)$ starts at the point $P(\frac{ck_p}{b}, O)$ for w = O and terminates at the point Q(O, O) for w = ∞. A typical Popov plot for a = 20, b = c = 25, and k_p = 1 is shown in Figure 4.

From equation (9), it is seen that $\omega\mathcal{I}mW(j\omega)$ is *always* negative for all non-zero w, that is, the Popov plot of $W(j\omega)$ remains entirely in the third and fourth quadrants and does *not* cross the real axis. This implies that we can construct a straight-line with a non-negative slope passing through the origin such that the Popov plot is entirely to the right of this line. Therefore, according to the Popov Criterion, the range of the allowable nonlinear gain k *is* **(0,00).**

4 Stability Analysis of Nonlinear PD Controllers

In this case, we employ the proportional-derivative (PD) controller

$$K(s) = k_p + k_d s \tag{lo}$$

in cascade with the nonlinear gain k, where k_p and k_d are the positive constant proportional and derivative gains, respectively.

To investigate the absolute stability of the closed-loop system, we combine the linear components (1) and (10) as

$$W(s) = G(s)K(s) = \frac{c(k_p + k_d s)}{s^2 + as + b} \tag{11}$$

which is a second-order transfer-function, and separate out the nonlinear element which is the gain k. To find out the range of values that the nonlinear gain k can assume while retaining closed-loop stability, we examine the Popov plot of $W(j\omega)$. In this case, from equation (11), we obtain

$$\mathcal{R}eW(j\omega) = \frac{c[(ak_d - k_p)\omega^2 + bk_p]}{a^2\omega^2 + (b-\omega^2)^2} \tag{12}$$

$$\omega\mathcal{I}mW(j\omega) = \frac{-c\omega^2[k_d\omega^2 + (ak_p - bk_d)]}{a^2\omega^2 + (b-\omega^2)^2} \tag{13}$$

The Popov plot of $W(j\omega)$ starts at the point $P(\frac{ck_p}{b}, O)$ for w = O and terminates at the point Q(O, $-ck_d$) for w = ∞. Two cases are now possible depending on the *relative* values of k_p and k_d.

4.1 Case One: $bk_d \leq ak_p$

In this case, from equation (13) it is seen that $\omega\mathcal{I}mW(j\omega)$ is *always* negative for all non-zero w, that is, the Popov plot of $W(j\omega)$ remains entirely in the third and fourth quadrants and does *not* cross the real axis. Therefore, according to the Popov Criterion, the range of the allowable nonlinear gain k is (O, cm). A typical Popov plot for a = 20, b = c = 25, k_p = 1, and k_d = 0.3 is shown in Figure 5a, and confirms the above analysis.

4.2 Case Two: $bk_d > ak_p$

In this case, the Popov plot of $W(j\omega)$ crosses the real axis. The crossover frequency ω_o is found by solving $\omega\mathcal{I}mW(j\omega) = O$ to yield

$$\omega_o^2 = \frac{bk_d - ak_p}{k_d} \tag{14}$$

and the value of $W(j\omega_o)$ is then found to be

$$\mathcal{R}eW(j\omega_o) = \frac{ck_d}{a} \tag{15}$$

which indicates that the Popov plot crosses the *positive* real axis in this case. The general shape of the Popov plot can be seen from a typical case shown in Figure 5b, where a = $20, b = c = 25, k_p = 1,$ and $k_d = 1$. It is seen that it is possible to construct a straight-line with a positive slope passing through the origin such that the Popov plot is entirely to the right of this line. Hence, from the Popov Criterion, the range of the allowable nonlinear gain k is (O, cm).

We conclude that in both cases, the closed-loop system is always stable under PD control with unbounded nonlinear gain k.

5 Stability Analysis of Nonlinear PI Controllers

In this case, the closed-loop system employs the proportional-integral (PI) controller

$$K(s) = k_p + \frac{k_i}{s} \tag{16}$$

in cascade with the nonlinear gain k, where k_p and k_i are the positive constant proportional and integral gains, respectively.

To investigate the absolute stability of the closed-loop system, we group the linear components (1) and (16) as

$$W(s) = G(s)K(s) = \frac{c(k_p s + k_i)}{s(s^2 + as + b)} \tag{17}$$

which is now a third-order transfer-function, and separate out the nonlinear element which is the gain k. To apply the Popov Stability Criterion stated in Section 3, we examine the Popov plot of $W(j\omega)$. This plot reveals the range of values that the nonlinear gain k can assume while retaining closed-loop stability. For this purpose, we need to compute the crossing of the Popov plot of $W(j\omega)$ with the real axis. In this case, from equation (17), we obtain

$$\mathcal{R}eW(j\omega) = \frac{-c[k_p\omega^2 + (sk_i - bk_p)]}{a^2\omega^2 + (b - \omega^2)^2} \tag{18}$$

$$\omega\mathcal{I}mW(j\omega) = \frac{-c[(ak_p - k_i)\omega^2 + bk_i]}{a2w2 + (b - W^2)^2} \tag{19}$$

The Popov plot of $W(j\omega)$ starts at the point $P(\frac{-c(ak_i - bk_p)}{b^2}, \frac{-ck_i}{b})$ for ω = O and ends at the point Q(O, O) for w = ∞. Two distinct cases are now possible depending on the relative values of k_i and k_p.

5.1 Case One: $k_i \leq ak_p$

In this case, $\omega\mathcal{I}mW(j\omega)$ is *always* negative for all w, that is, the Popov plot of $W(j\omega)$ remains entirely in the third and fourth quadrants and does *not* cross the real axis. This implies that we can construct a straight-line with a non-negative slope passing through the origin such that the Popov plot is entirely to the right of this line. Therefore, according to the Popov Criterion, the range of the allowable nonlinear gain k is (O, 00). A typical Popov plot in this case is given in Section 7.

5.2 Case Two: $k_i > ak_p$

In this case, the Popov plot of $W(j\omega)$ crosses the real axis. The crossover frequency ω_o is found by solving $\omega\mathcal{I}mW(j\omega) = O$ to yield

$$W^{*2} = \frac{bk_i}{k_i - ak_p} \tag{20}$$

The value of $W(j\omega)$ at the crossover is then obtained as

$$\mathcal{R}eW(j\omega_o) = \frac{(ak_p - k_i)c}{ab} \tag{21}$$

indicating that the Popov plot crosses the negative real axis in this case. Therefore, the *maximum* allowable nonlinear gain is

$$k_{max} = \frac{1}{\mathcal{R}eW(j\omega_o)} = \frac{ab}{(k_i - ak_p)c} \tag{22}$$

We can now construct a straight-line with anon-negative slope passing through the point $-\frac{1}{k_{max}} + j0$ such that the Popov plot of $W(j\omega)$ is entirely to the right of this line. Thus the range of the allowable nonlinear gain k is (O, k_{max}). A typical Popov plot in this case is given in Section 7.

Observe that the distinction between the above two cases is on the *relative* values of the proportional and integral gains k_p and k_i in the PI controller, and not on their absolute values. Notice that a reasonable estimate of the attenuation factor a of the transfer-function (1) can readily be obtained experimentally from the open-loop response of the output y to the step control input u. Specifically, the step response has the settling time of $t_s = \frac{5}{\xi\omega} = \frac{10}{a}$ to reach within the $\pm 1\%$ tolerance band of its final value [2].

6 Stability Analysis of Nonlinear PID Controllers

In this case, we employ the proportional-integral-derivative (PID) controller

$$K(s) = k_p + \frac{k_i}{s} + k_d s \tag{23}$$

in cascade with the nonlinear gain k, where k_p, k_i, and k_d are the positive constant proportional, integral, and derivative gains, respectively.

To investigate the absolute stability of the closed-loop system, we combine the linear components (1) and (23) as

$$W(s) = G(s)K(s) = \frac{c(k_d s^2 + k_p s + k_i)}{s(s^2 + as + b)} \tag{24}$$

which is a third-order transfer-function, and separate out the nonlinear element which is the gain k. In order to assess the stability of the closed-loop system, we examine the Popov plot of $W(j\omega)$. This plot reveals the range of values that the nonlinear gain k can assume while retaining closed-loop stability. In this case, from equation (24), we obtain

$$\mathcal{R}eW(j\omega) = \frac{-C[(k_p - ak_d)\omega^2 + (ak_i - bk_p)]}{a2w2 + (b-\omega^2)^2} \tag{25}$$

$$\omega\mathcal{I}mW(j\omega) = \frac{-c[k_d\omega^4 + (ak_p - bk_d - k_i)\omega^2 + bk_i]}{a^2\omega^2 + (b-\omega^2)^2} \tag{26}$$

The Popov plot of $W(j\omega)$ starts at the point $P(\frac{-c(ak_i - bk_p)}{b^2}, \frac{ck_i}{b})$ for w = O and ends at the point Q(O, $-ck_d$) for w = ∞. To apply the Popov Criterion, we need to compute the crossing of the Popov plot of $W(j\omega)$ with the real axis. From equation (26), it is clear that when $(ak_p - bk_d - k_i) \geq 0$ o r

$$bk_d + k_i \leq ak_p \tag{27}$$

then $\omega\mathcal{I}mW(j\omega)$ is negative *for all w*, thus the Popov plot does not cross the real axis. In this case, the range of the nonlinear gain k for stability is (O, cm). Hence equation (27) gives a *sufficient*, but not a necessary, condition for closed-loop stability for all values of k.

When $bk_d + k_i > ak_p$, the closed-loop system may become unstable for some values of k. These values of k correspond to the cases where the Popov plot crosses the real axis, that is, $\omega\mathcal{I}mW(j\omega) = O$. In the Appendix, the conditions under which this equation has positive real roots are found. Two distinct cases are possible depending on the *relative* values of k_p, k_i, and k_d.

6.1 Case One: $\sqrt{ak_p} > |\sqrt{bk_d} - \sqrt{k_i}|$

In this case, equation (26) cannot have positive real roots for w. Hence the Popov plot of $W(j\omega)$ does not cross the real axis and stays entirely in the third and fourth quadrants. Therefore, according to the Popov Criterion, the range of the allowable nonlinear gain k is (O, ∞). A typical Popov plot for a = 20, b = c = 25, $k_p = 1$, $k_i = 1$, and $k_d = 0.5$ is shown in Figure 6, and confirms the above analysis.

6.2 Case Two: $\sqrt{ak_p} \leq |\sqrt{bk_d} - \sqrt{k_i}|$

In this case, the Popov plot of $W(j\omega)$ crosses the real axis. Equation (26) now has two positive real roots ω_1 and ω_2, with WI < ω_2, which are the two crossover frequencies. These frequencies are the roots of the following equation:

$$k_d\omega^4 i\text{-} (ak_p - bk_d - k_i)\omega^2 + bk_i = O \tag{28}$$

which can be factored as:

$$(k_d\omega^2 - k_i)(\omega^2 - b) + ak_p\omega^2 = 0 \tag{29}$$

The values of $W(j\omega)$ at the two crossovers are then found from equation (25) as

$$\mathcal{R}eW(j\omega_i) = \frac{c[a(k_d\omega_i^2 - k_i) - k_p(\omega_i^2 - b)]}{a^2\omega_i^2 + (b - \omega_i^2)^2} \tag{30}$$

for $i=1$, 2. Substituting for $(\omega_i^2 - b)$ from equation (29) into equation (30) and simplifying the result yields the surprisingly simple expression

$$\mathcal{R}eW(j\omega_i) = \frac{ck_p}{b - \omega_i^2} \tag{31}$$

Now, for the Popov plot to cross the *negative* real axis, we need to find the condition under which $b < \omega_i^2$. Consider the polynomial

$$g(\omega^2) = k_d\omega^4 + (ak_p - bk_d - k_i)\omega^2 + bk_i \tag{32}$$

where the plot of $g(\omega^2)$ versus ω^2 is a parabola that crosses the ω^2-axis at ω_1^2 and ω_2^2. Since $k_d > 0$, for any value of ω^2 "inside" the parabola, the expression $g(\omega^2)$ is negative, while for all values of ω^2 "outside" the parabola (including the origin ω^2 = O), the expression $g(\omega^2)$ is positive. For $\omega^2 = b$, we have $g(b) = abk_p > 0$, hence $\omega^2 = b$ is located outside the parabola, that is, either $b < \omega_1^2 < \omega_2^2$ or $\omega_1^2 < \omega_2^2 < b$. To find out the condition for the former case to occur, we only need to compare the location of the midpoint $\omega_o^2 = \frac{\omega_1^2 + \omega_2^2}{2}$ *relative* to b. In order for $b < \omega_i^2$, we need $b < \omega_o^2$. Using the sum-of-roots relationship for equation (28) yields

$$b < -\frac{ak_p - bk_d - k_i}{2k_d} \tag{33}$$

which simplifies to

$$ak_p + bk_d < k_i \tag{34}$$

We conclude that when $\sqrt{ak_p} \leq |\sqrt{bk_d} - \sqrt{k_i}|$ and $ak_p + bk_d < k_i$, the **Popov plot of** $W(j\omega)$ crosses the *negative* real axis $[\mathcal{R}eW(j\omega_i) < O]$, and the nonlinear gain k must be upper-bounded by

$$k_{max} = -\frac{1}{\mathcal{R}eW(j\omega_1)} = \frac{\omega_1^2 - b}{ck_p} \tag{35}$$

to ensure closed-loop stability, that is, O < k < k_{max}. Notice that since $\omega_1^2 < \omega_o^2$, from equation (35) the maximum nonlinear gain is bounded by

$$k_{max} < \frac{k_i - ak_p - bk_d}{2ck_pk_d} \tag{36}$$

A typical Popov plot in this case is given in Section 7.

On the other hand, when $\sqrt{ak_p} \leq |\sqrt{bk_d} - \sqrt{k_i}|$ but $ak_p + bk_d \geq k_i$, the Popov plot of $W(j\omega)$ crosses the *positive* real axis $[\mathcal{R}eW(j\omega_i) > O]$, and the general shape of the Popov plot

can be seen from a typical case given in Section 7. It is seen that it is possible to construct a straight-line with a positive slope passing through the origin such that the Popov plot is entirely to the right of this line. Hence from the Popov Criterion the nonlinear gain k is unbounded, that is, $O < k < \infty$.

From the condition $ak_p + bk_d < k_i$, we observe that the effect of the derivative gain k_d is to increase the range of the integral gain k_i for stability. Notice that when $k_d = O$, the result of Section 5 for PI controllers, namely $ak_p < k_i$, is obtained.

7 Illustrative Example

For the sake of illustration, computer simulations of the Popov plot for a robotic manipulator with nonlinear PI and PID controllers are presented. Given the end-effecter transfer-function

$$G(s) = \frac{25}{s^2 + 20s + 25} \tag{37}$$

we investigate the stability of the closed-loop system using nonlinear controllers.

7.1 Nonlinear PI Controller

Using the fixed-gain PI controller

$$K(s) = k_p + \frac{2}{s} \tag{38}$$

in cascade with the nonlinear gain k, the Popov plots of $W(s) = G(s)K(s)$ for the two values of the proportional gain $k_p = 2$ and $k_p = O$ are shown in Figures 7a-7b. For $k_p = 2$, it is seen from Figure 7a that the Popov plot of $W(j\omega)$ does not cross the real axis as expected; hence the allowable range of the nonlinear gain k is (O, cm). In contrast, when k_p is reduced to zero, Figure 7b reveals that the Popov plot of $W(j\omega)$ crosses the real axis at –0.1, hence the allowable range of k is now reduced to (O, 10). These results agree with the findings in Section 5.

We conclude that increasing k_p in the PI controller has a stabilizing effect and increases the range of the allowable nonlinear gain k to maintain closed-loop stability.

7.2 Nonlinear PID Controller

In this case, we employ the fixed-gain PID controller

$$K(s) = 0.25 + \frac{6}{s} + k_d s \tag{39}$$

in cascade with the nonlinear gain k. The Popov plots of $W(s) = G(s)K(s)$ for the two values of the derivative gain $k_d = O$ and $k_d = 2$ are obtained, as shown in Figures 8a-8b.

From Figure 8a, it is seen that when $k_d = O$, the Popov plot crosses the negative real axis at -0.05; hence the allowable range of the nonlinear gain kis (0,20). On the other hand, when k_d is increased to $k_d = 2$, the Popov plot in Figure 8b indicates that the *positive* real axis is now crossed, and the range of the nonlinear gain k is now (O, cm). These results are in agreement with those derived in Section 6.

We conclude that increasing k_d in the PID controller has a stabilizing effect and increases the range of the nonlinear gain k for maintaining closed-loop stability.

8 Conclusions

It is widely believed that a "perfect" control system must exhibit a fast response with no overshoot. These two requirements are contradictory when linear controllers are used, and are often impossible to achieve when the system operating conditions undergo gross variations. A fast response requires a large gain which, in turn, gives rise to a large overshoot, manifesting the contradiction of the two requirements. This paper proposes a simple solution to this fundamental problem by enhancing a fixed-gain PID controller with a nonlinear gain k. The nonlinear characteristics of the gain enables the achievement of fast initial response when k is large, followed by a small overshoot when k is small. Thus the nonlinear PID controller does not suffer from the disadvantage of large overshoots which often accompany a fast response. This automatic adjustment of the gain is the main advantage of the nonlinear PID controller over the conventional linear PID controller.

Current research is aimed at the implementation and practical validation of the proposed nonlinear PID control schemes in robotic compliance and force control applications.

9 Acknowledgments

The research described in this paper was carried out at the Jet Propulsion Laboratory, California Institute of Technology, under contract with the National Aeronautics and Space Administration. The author wishes to thank Dr. Robert Bonitz of JPL for the simulation environment used in Section 2 and for his constructive comments on the paper.

10 Appendix

Consider the quadratic equation

$$AX^2 + BX + C = 0 \tag{40}$$

where the coefficients A, B, and C are constants, and A and C are known to be positive. We wish to find the conditions on A, B, and C under which equation (40) will have two positive real roots. Clearly, if the coefficient B is zero or positive, for any positive number X, the

expression $(AX^2 + BX + C)$ is positive. Hence, a *sufficient*, but not a necessary, condition for not having a positive real root is $B \geq$ O. Now, since the product-of-roots of equation (40) is positive, this equation can only have either two positive real or two negative real roots. Let A = B^2 – 4AC be the discriminant. Then the conditions for existence of two positive real roots are:

$$\Delta \geq 0 \quad ; \quad B < 0 \tag{41}$$

The first condition yields

$$(B - 2\sqrt{AC})(B + 2\sqrt{AC}) \geq 0 \tag{42}$$

Since $(B - 2\sqrt{AC})$ is negative in view of equation (41), the required condition becomes

$$B \leq -2\sqrt{AC} \tag{43}$$

Therefore, when $B > -2\sqrt{AC}$, equation (40) will *not* have two positive real roots.

To apply this result to the nonlinear PID controller in Section 6, we substitute: $A = k_d$, $B = ak_p - bk_d - k_i$, $C = bk_i$. This yields

$$ak_p - bk_d - k_i \leq -2\sqrt{bk_dk_i} \tag{44}$$

Hence, the required condition for the Popov plot to cross the real axis is found to be

$$ak_p \leq (\sqrt{bk_d} - \sqrt{k_i})^2 \tag{45}$$

This equation yields the condition for real axis crossing as

$$\sqrt{ak_p} \leq |\sqrt{bk_d} - \sqrt{k_i}| \tag{46}$$

Therefore, when $\sqrt{ak_p} > |\sqrt{bk_d} - \sqrt{k_i}|$, the Popov plot does *not* cross the real axis.

11 References

1. Y. Xu, J .M. Hollerbach, and D. Ma: "A nonlinear PD controller for force and contact transient control", IEEE Control Systems Magazine, pp. 15-21, 1995.

2. K. Ogata : *Modern Control Engineering*, Prentice-Hall Inc., Englewood Cliffs, N. J., 1970.

3. H. Seraji, B. Bon, and R. Steele: "Experiments in real-time collision avoidance for dexterous 7-DOF arms", Proc. IEEE Intern. Conf. on Robotics and Automation, Albuquerque, 1997.

4. K.S. Narendra and J.H. Taylor: *Frequency Domain Criteria for Absolute Stability*, Academic Press Publishers, New York, 1973.

5. M. Vidyasagar: *Nonlinear Systems Analysis*, Prentice-Hall Inc., Englewood Cliffs, N. J., 1978.

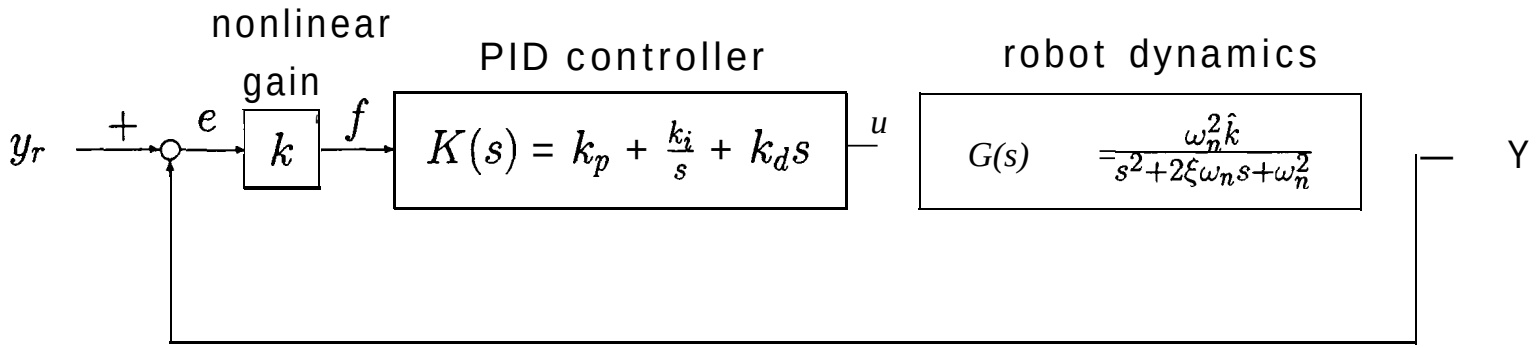

Figure 1a: Block diagram of nonlinear PID control system

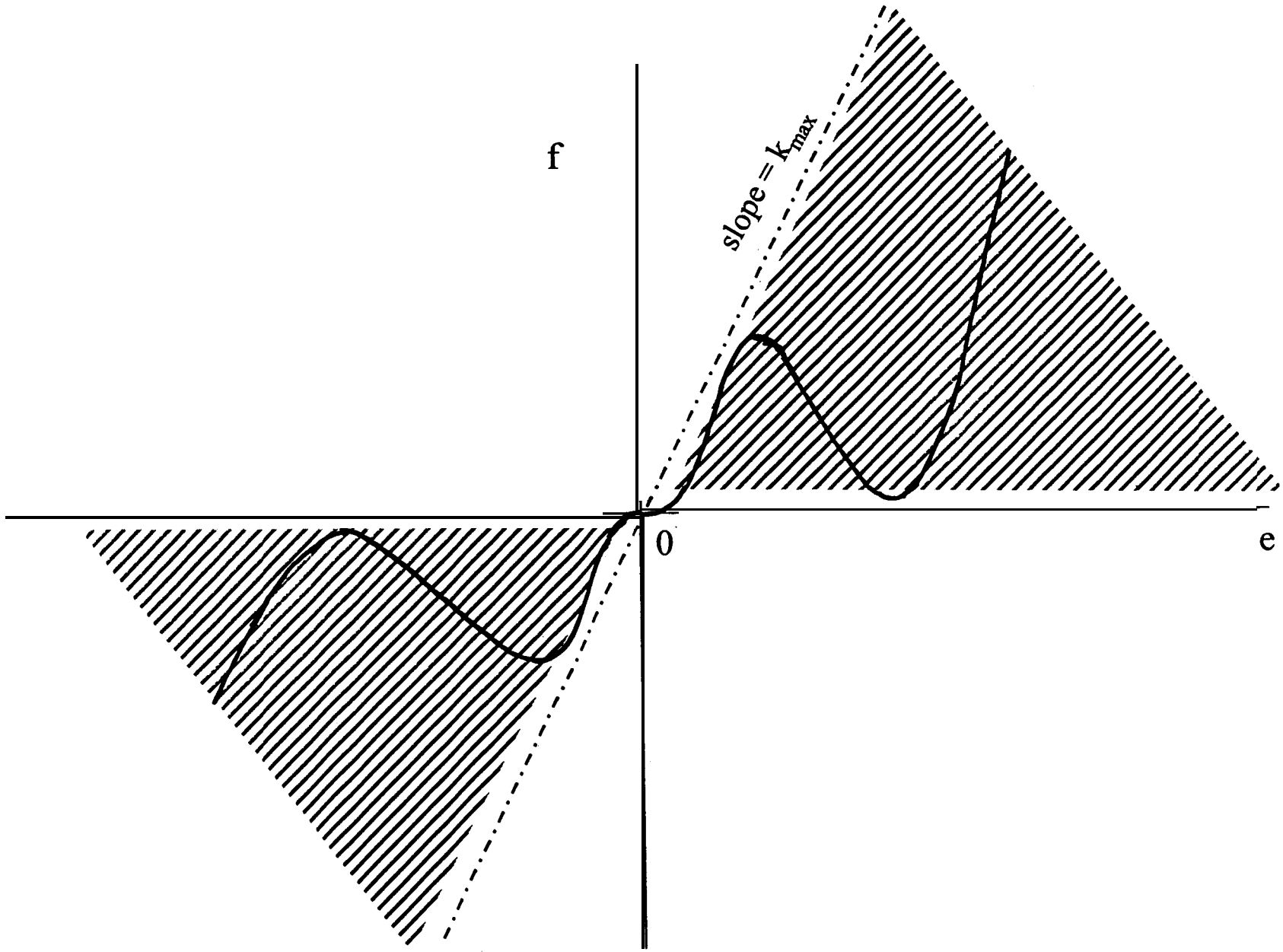

Figure 1b: Input-output characteristic of the nonlinear gain

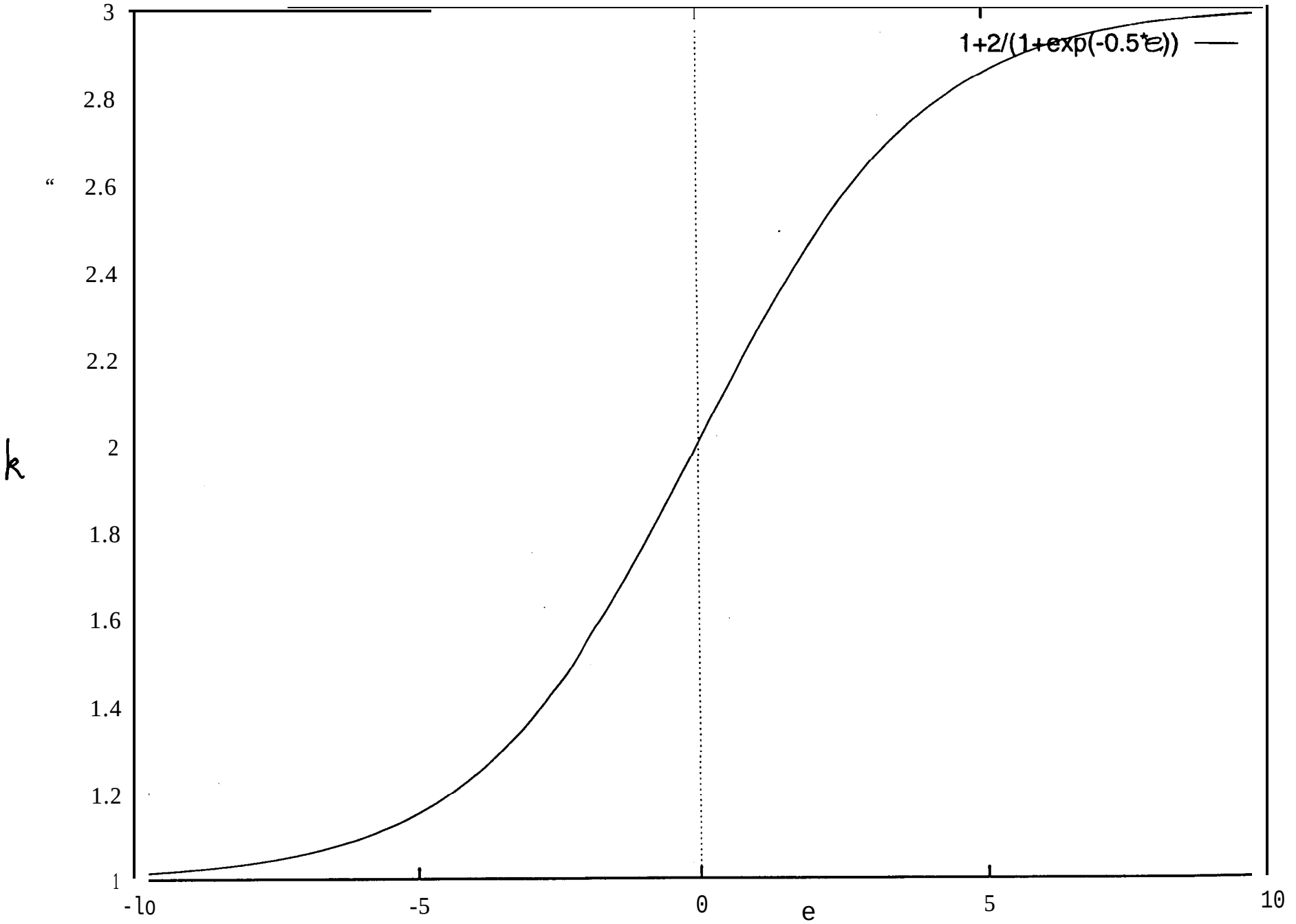

Figure 2a: Variation of the gain k as a **sigmoidal function** of the error e

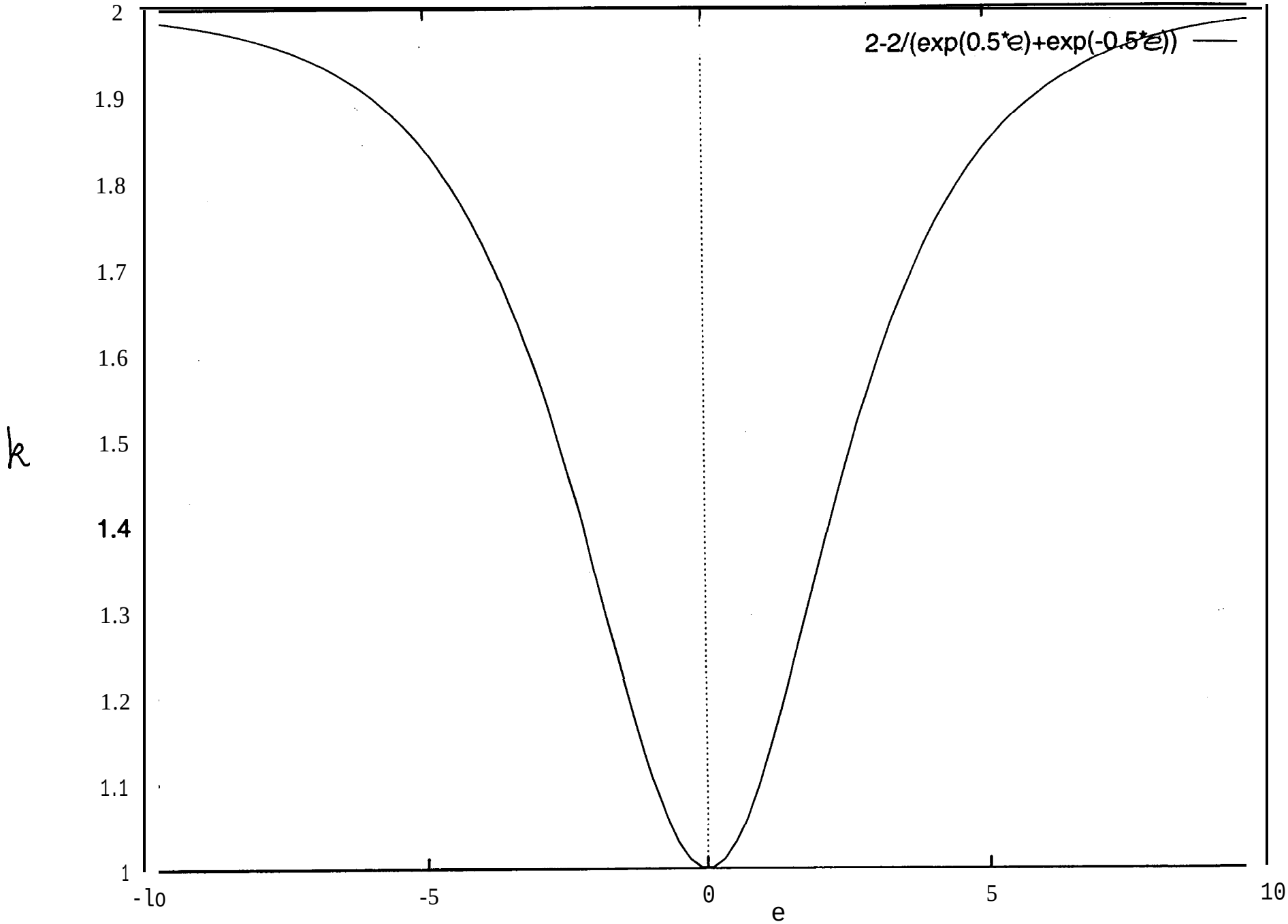

Figure 2b: Variation of the gain **k as** a hyperbolic **function** of the error e

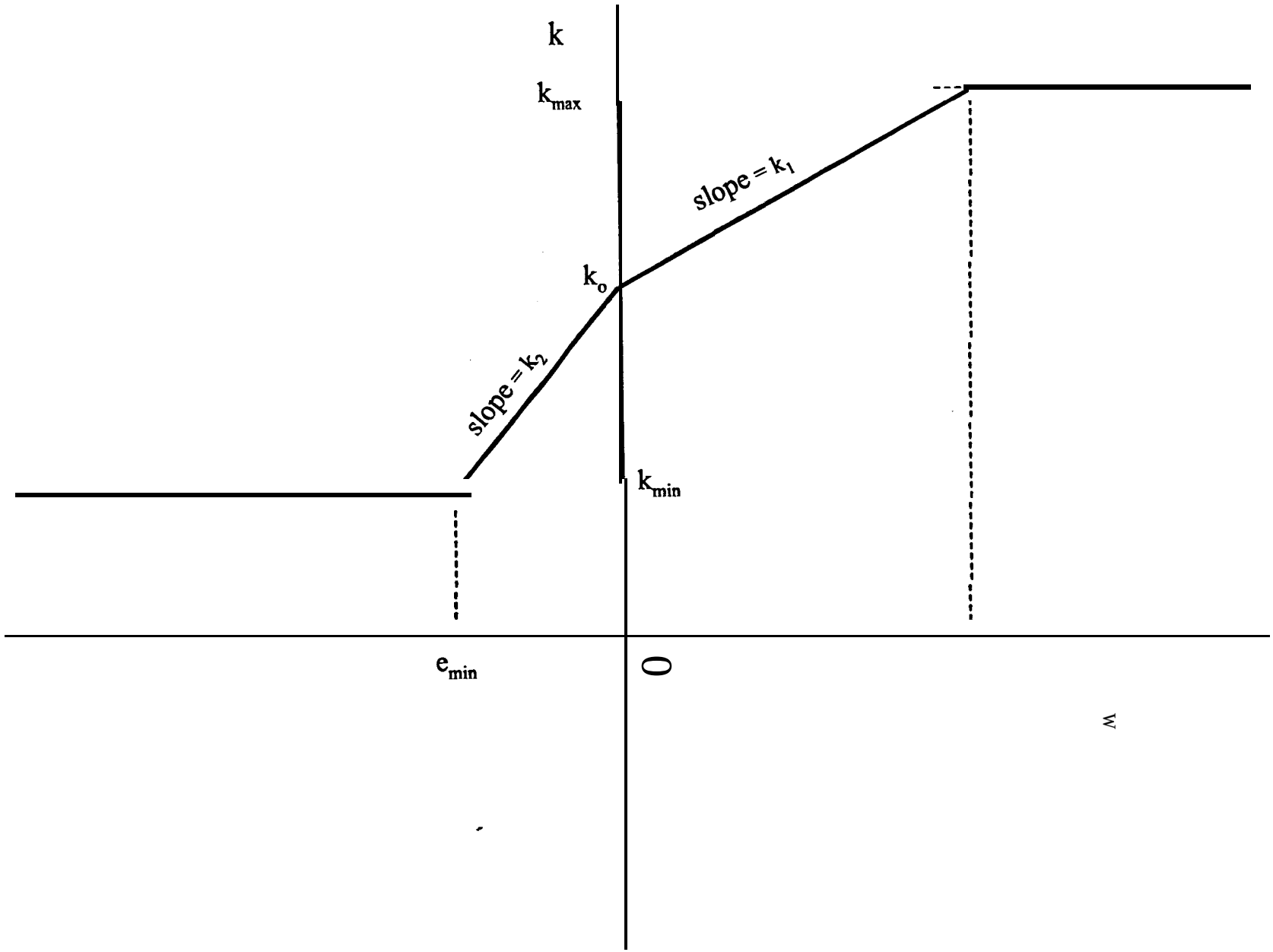

Figure 2c: Variation of the gain k as a p w function of the error e

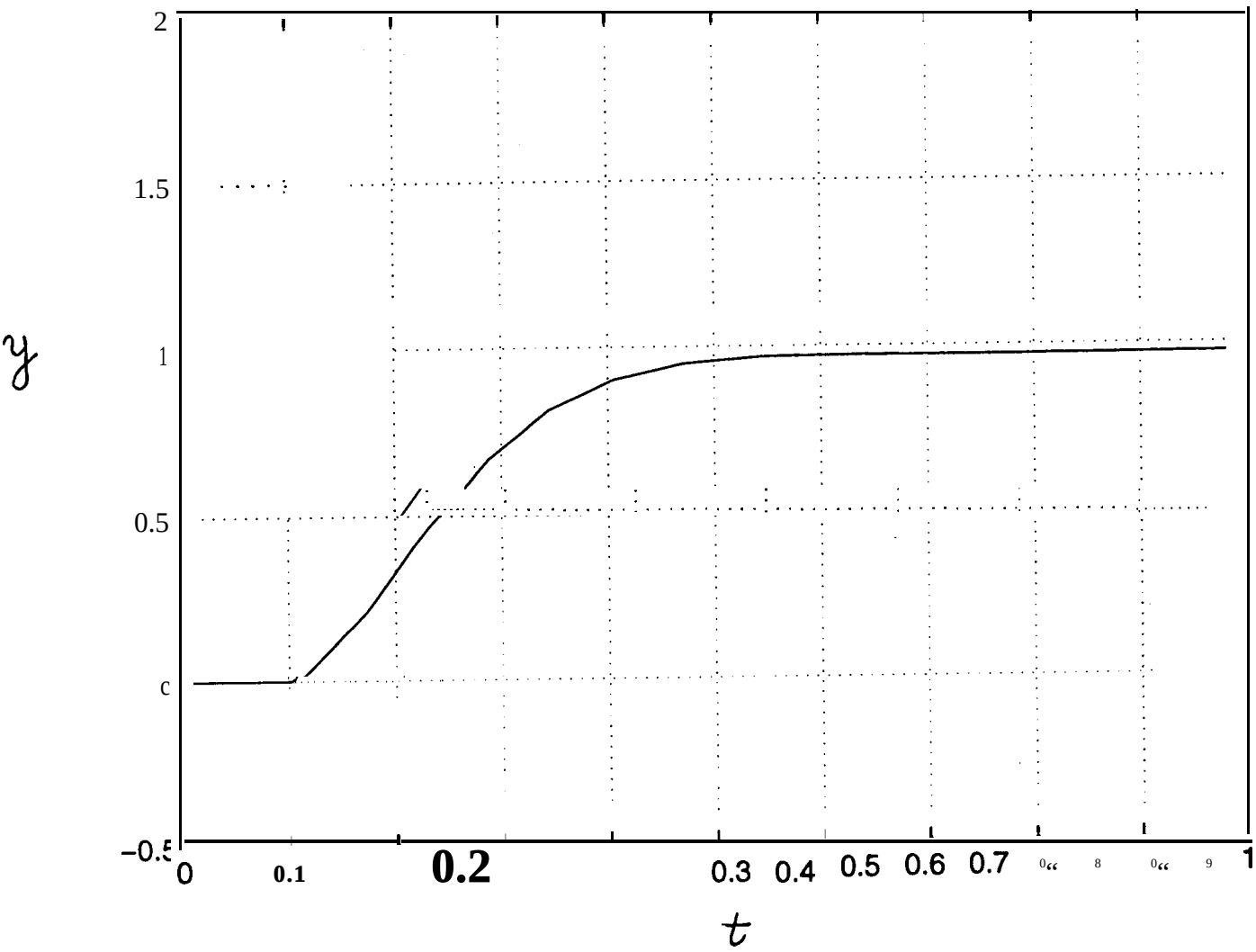

Figure 3a: Closed-loop step response using the fixed-gain PI controller

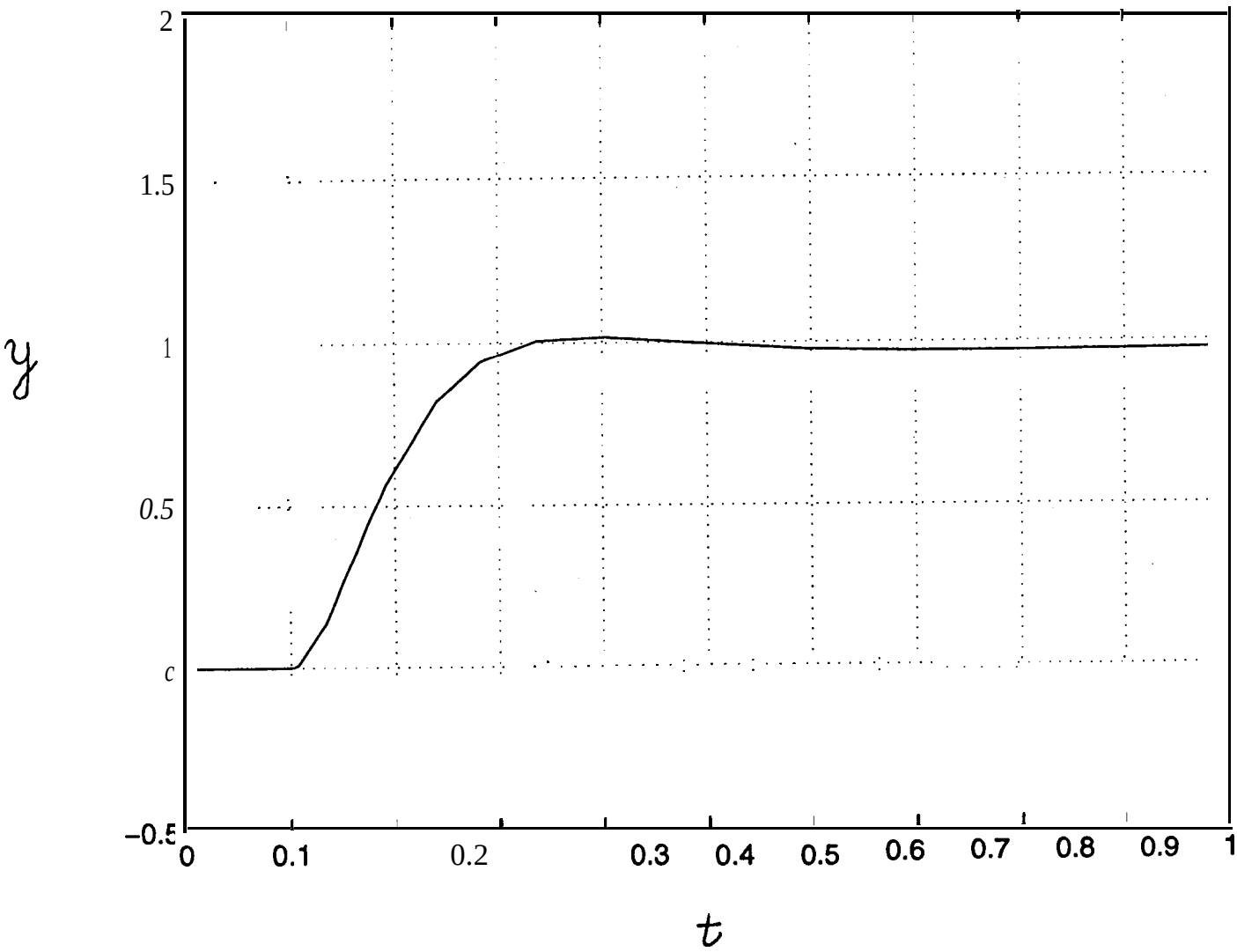

Figure 3b: Closed-loop step response using the nonlinear gain PI controller

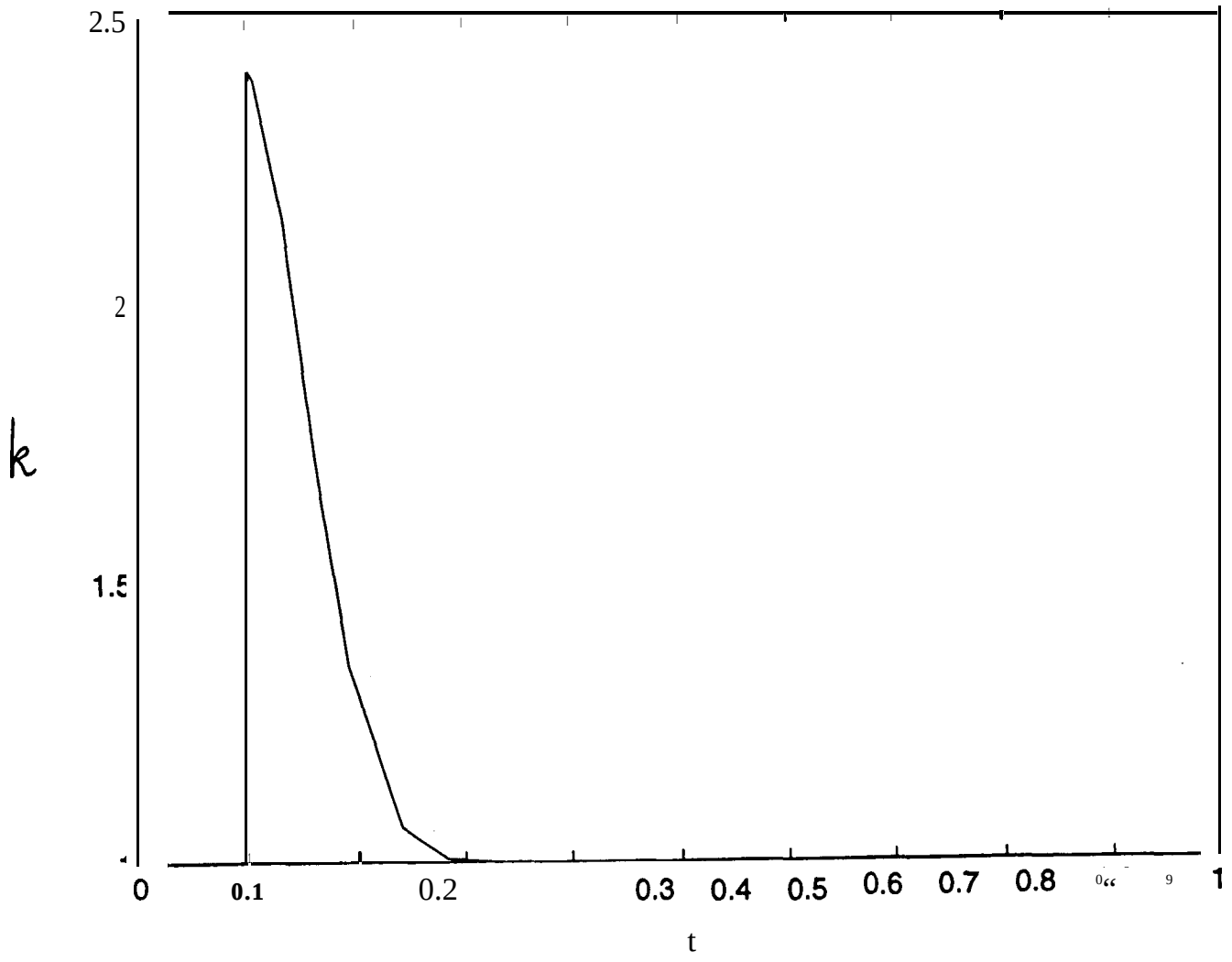

Figure 3c: Variation of the nonlinear gain with time

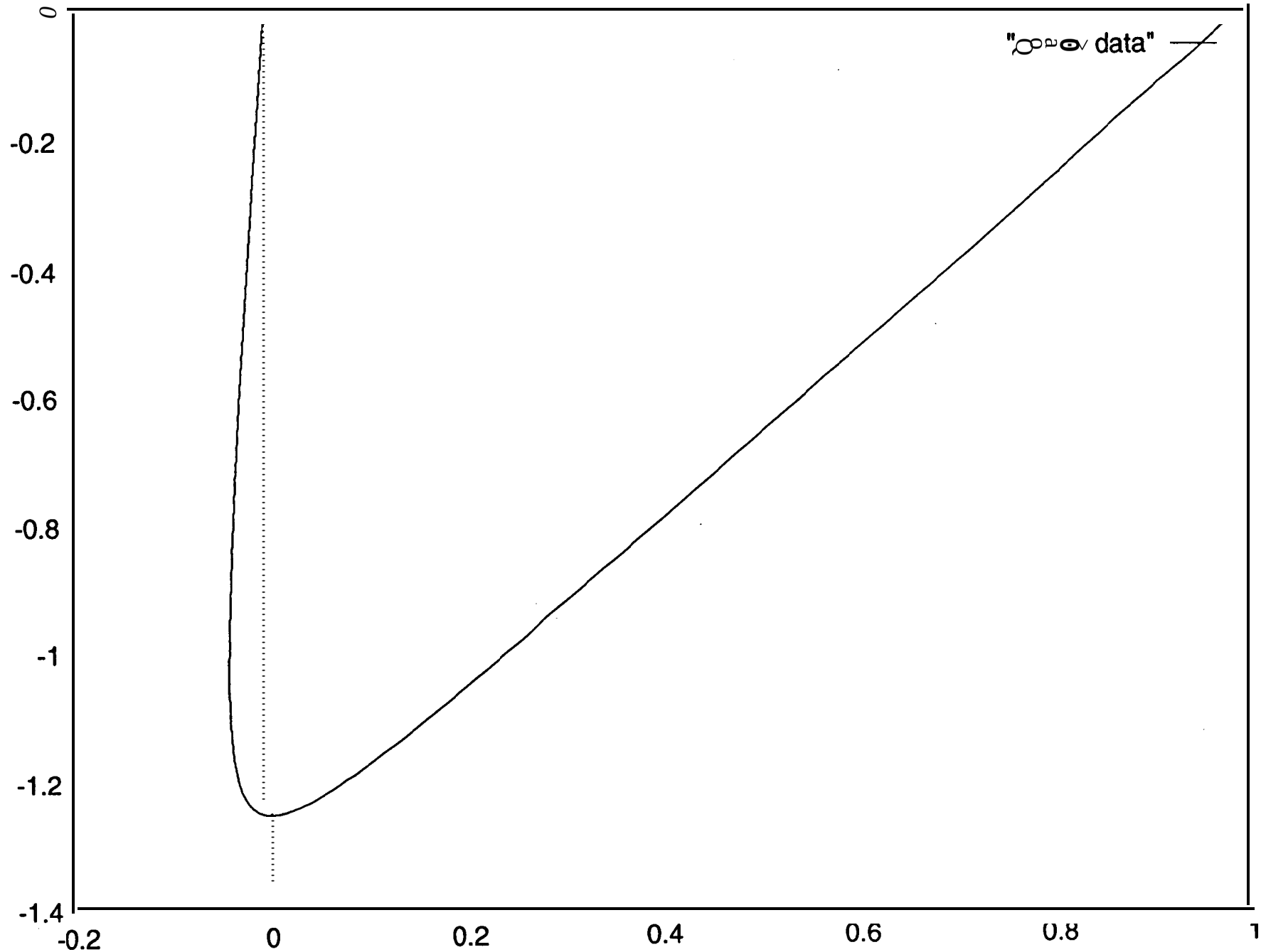

Figure 4: Popov plot for the nonlinear P-controlled system

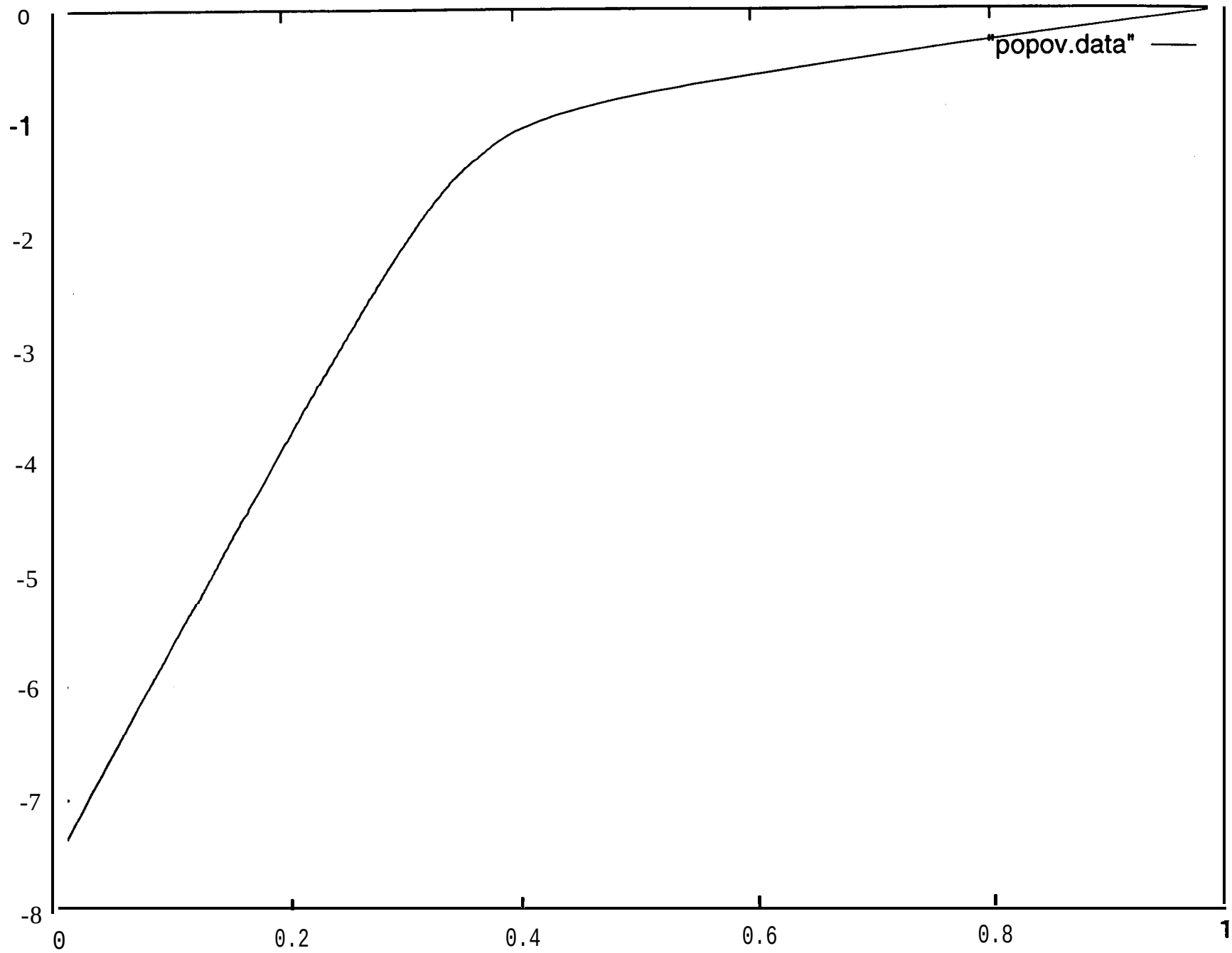

Figure 5a: **Popov** plot for the nonlinear **PD-controlled** system - Case One

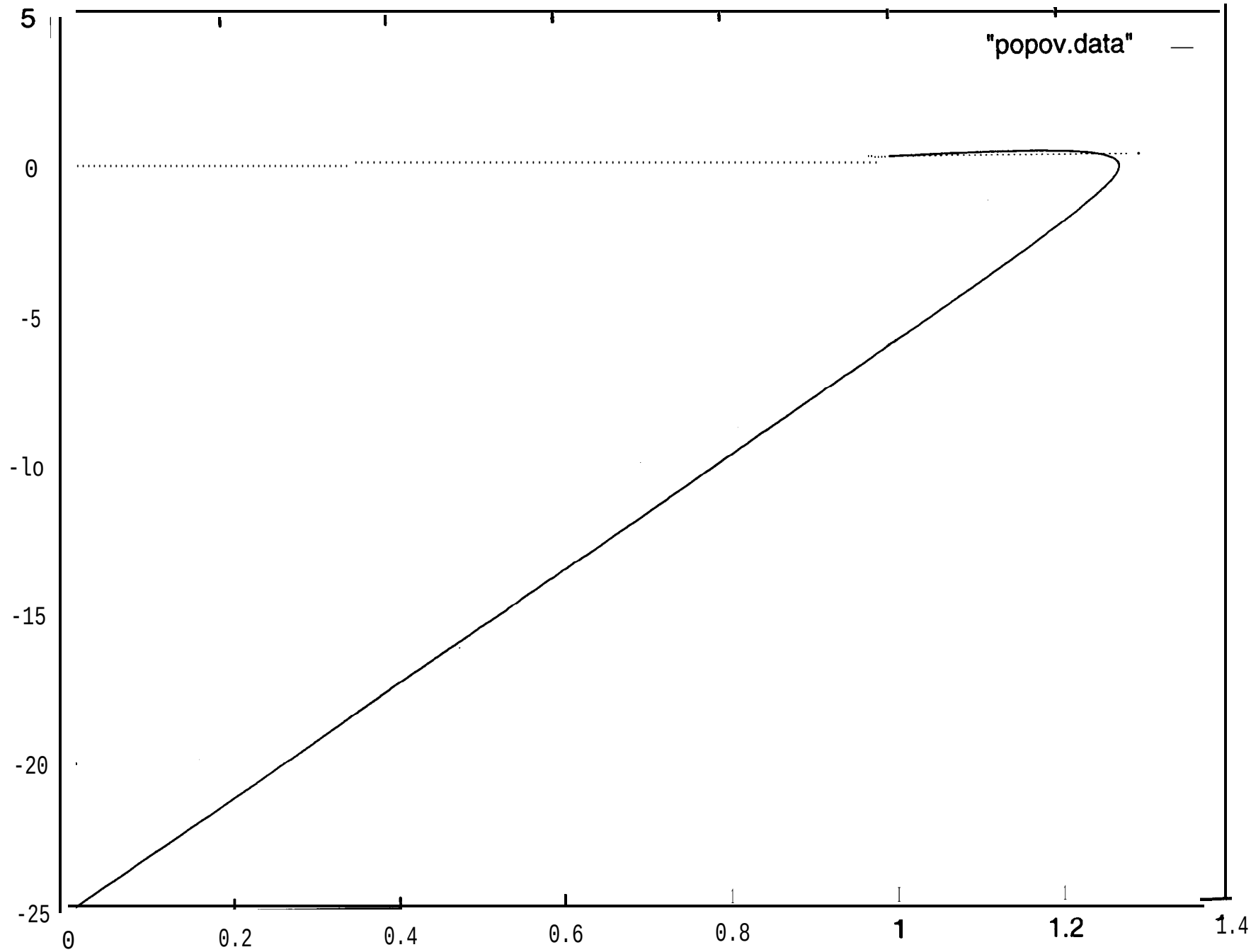

Figure 5b: Popov plot for the nonlinear **PD-controlled** system - Case Two

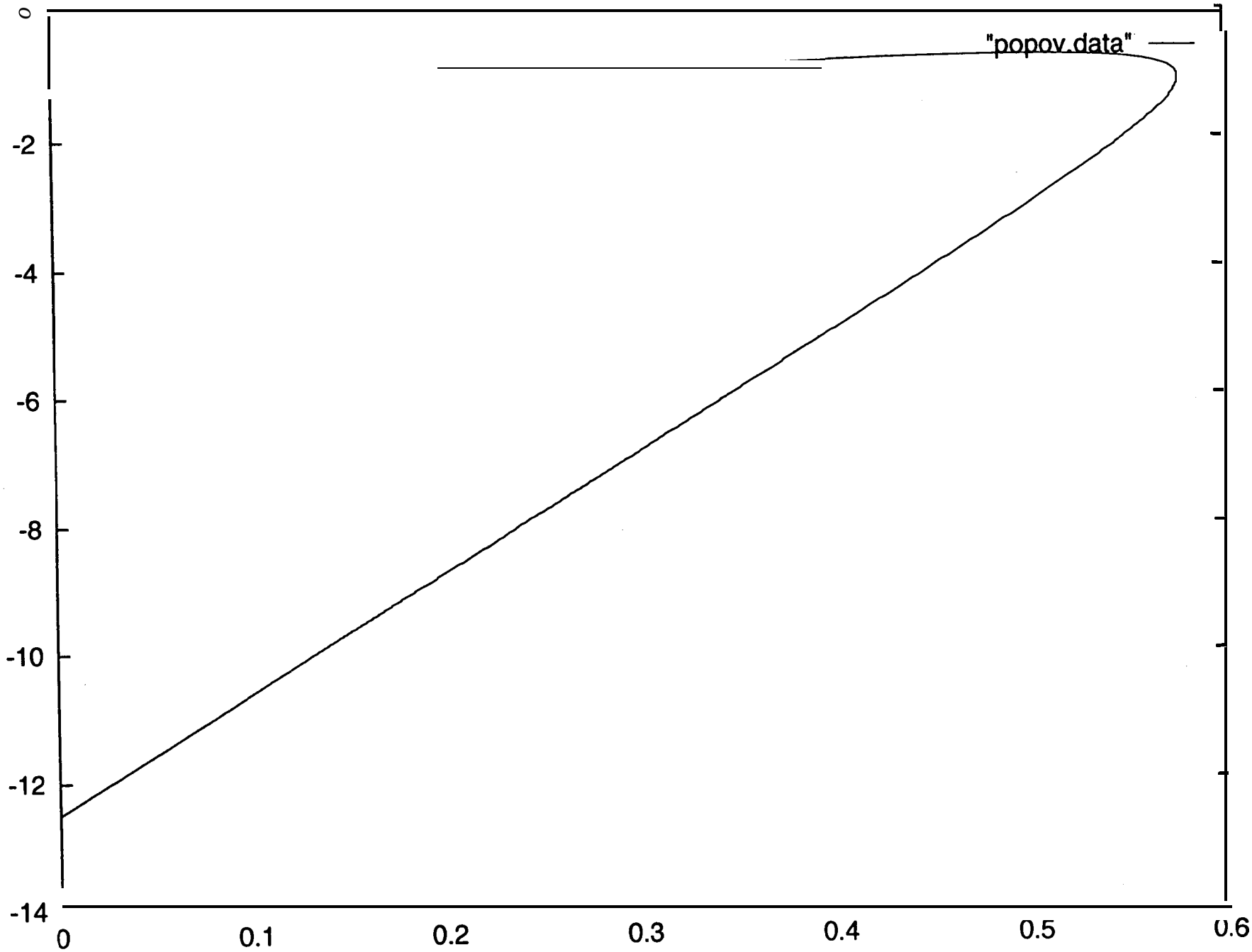

Figure 6: Popov plot for the nonlinear PID-controlled system

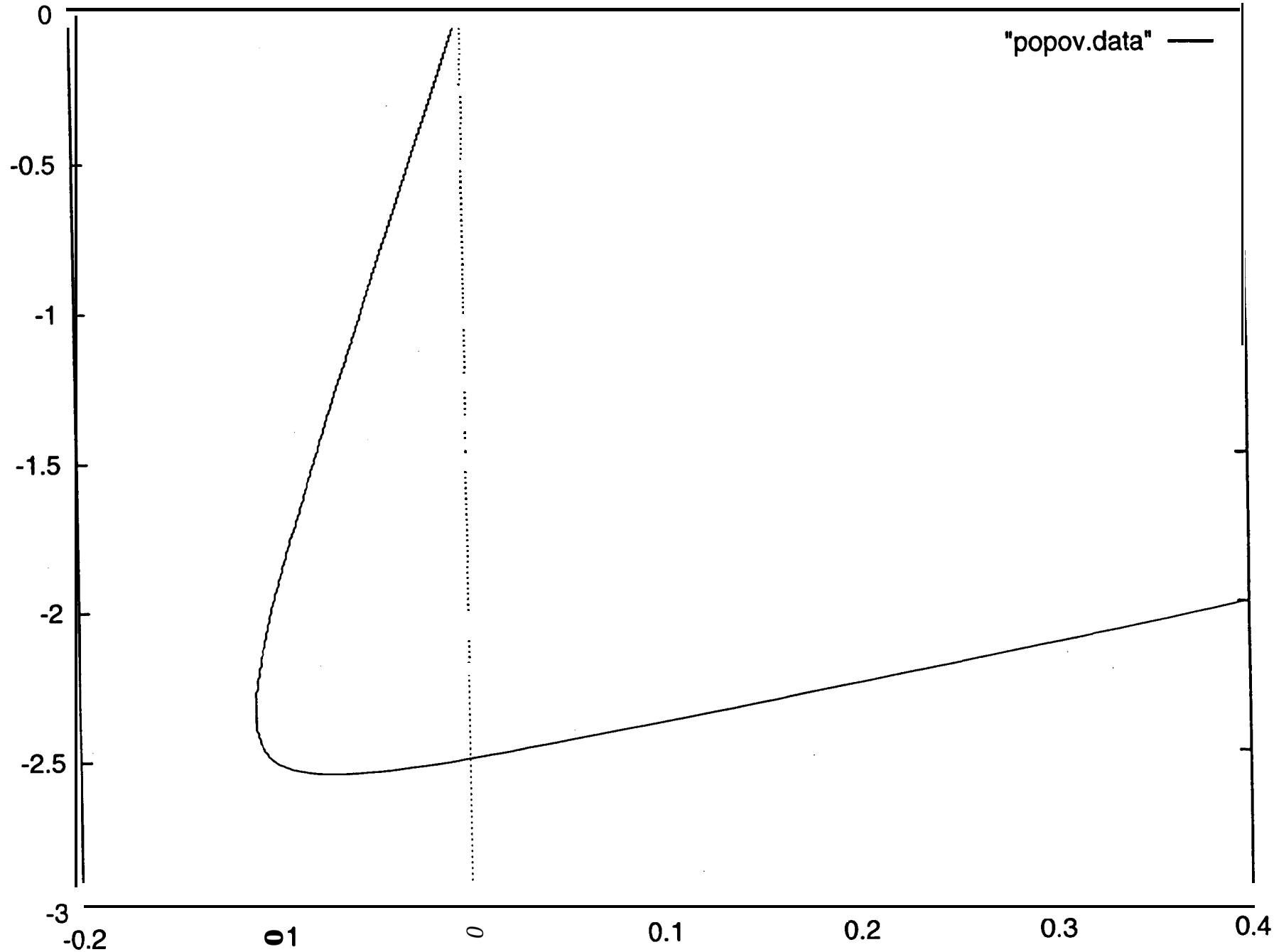

Figure 7a: Popov plot for h nonlinear PI-controlled system with $k_p = 2$

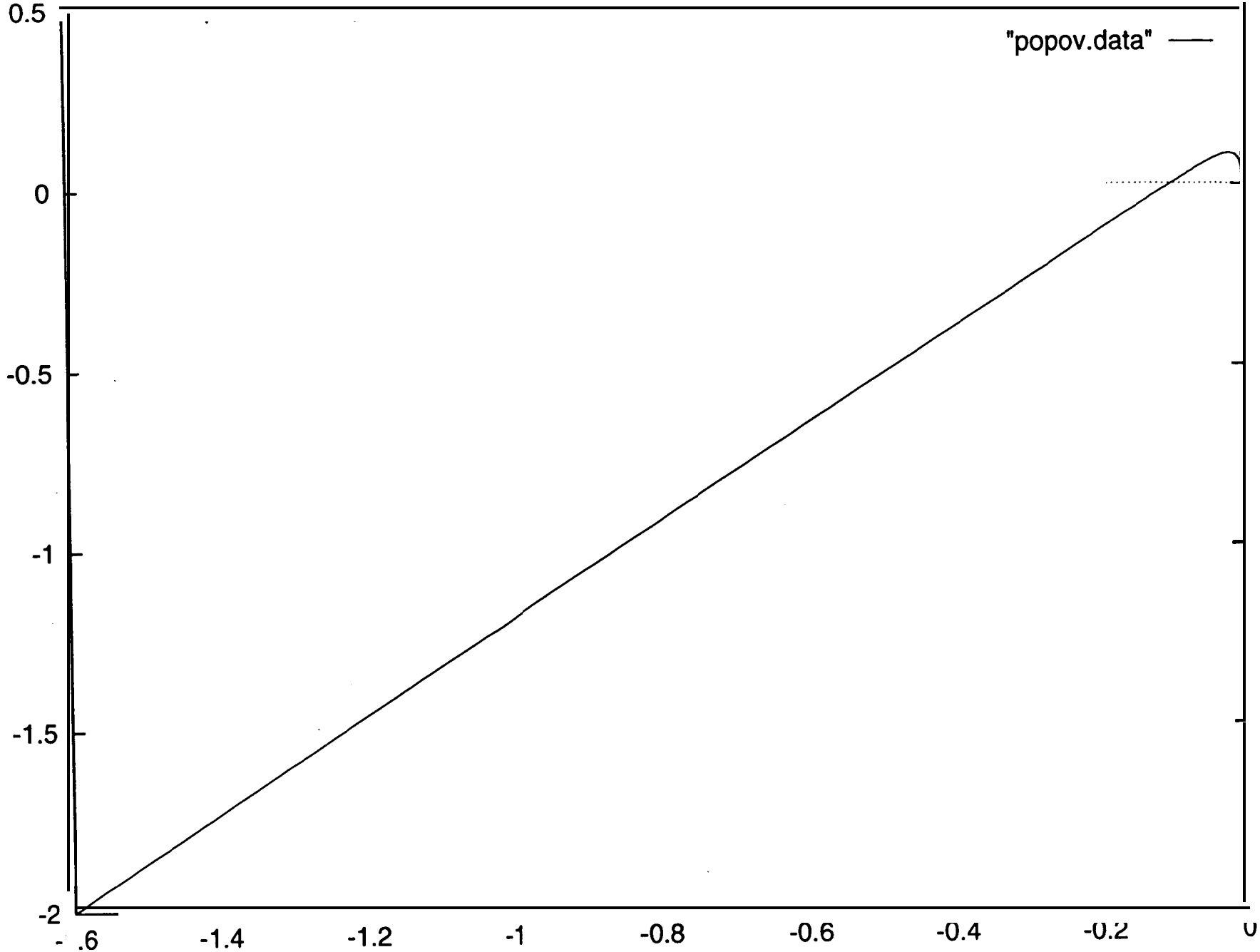

Figure 7b: Popov plot for the nonlinear PI-controlled system with $k_p = 0$

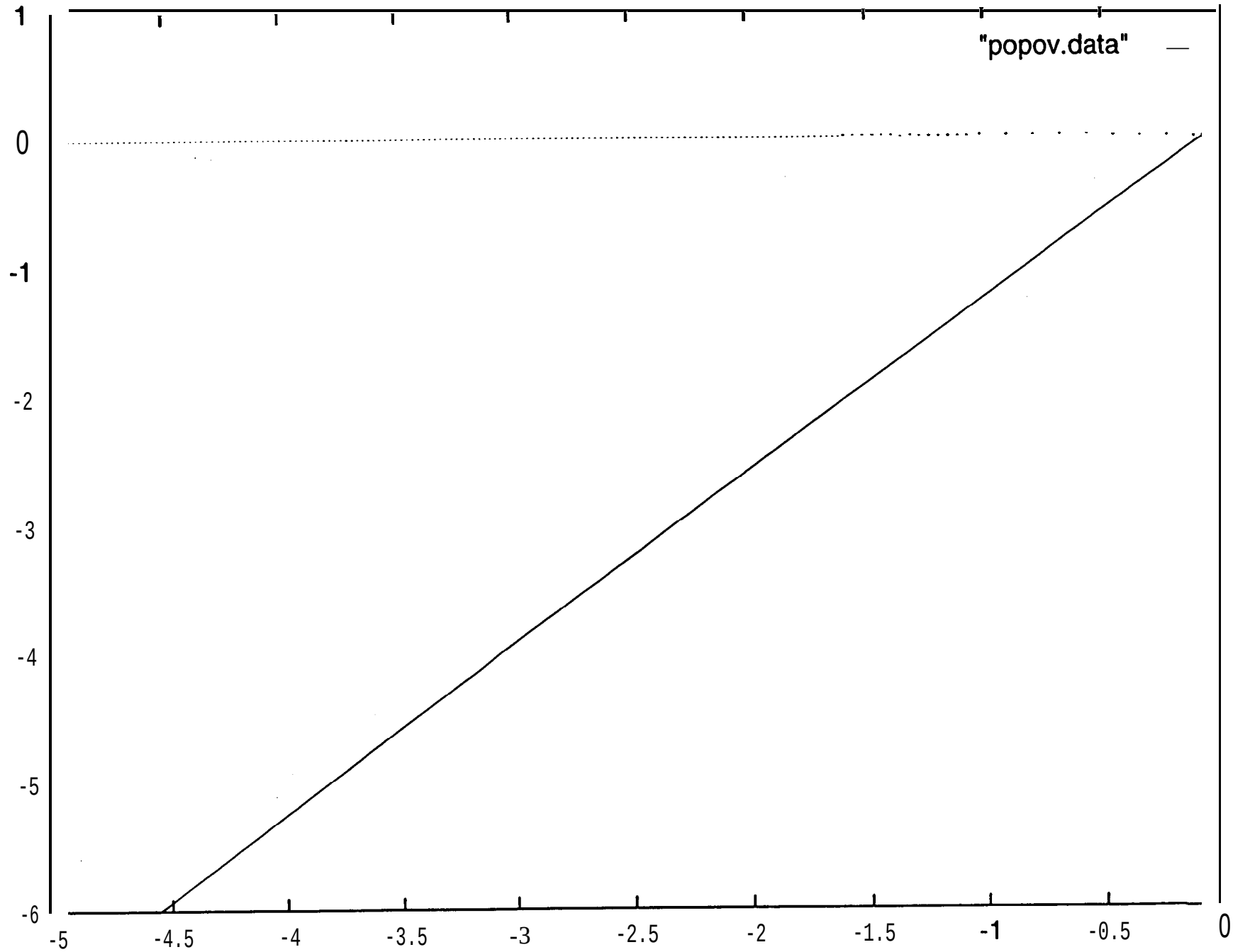

Figure 8a: Popov plot for the nonlinear **PID-controlled** system with $k_d = 0$

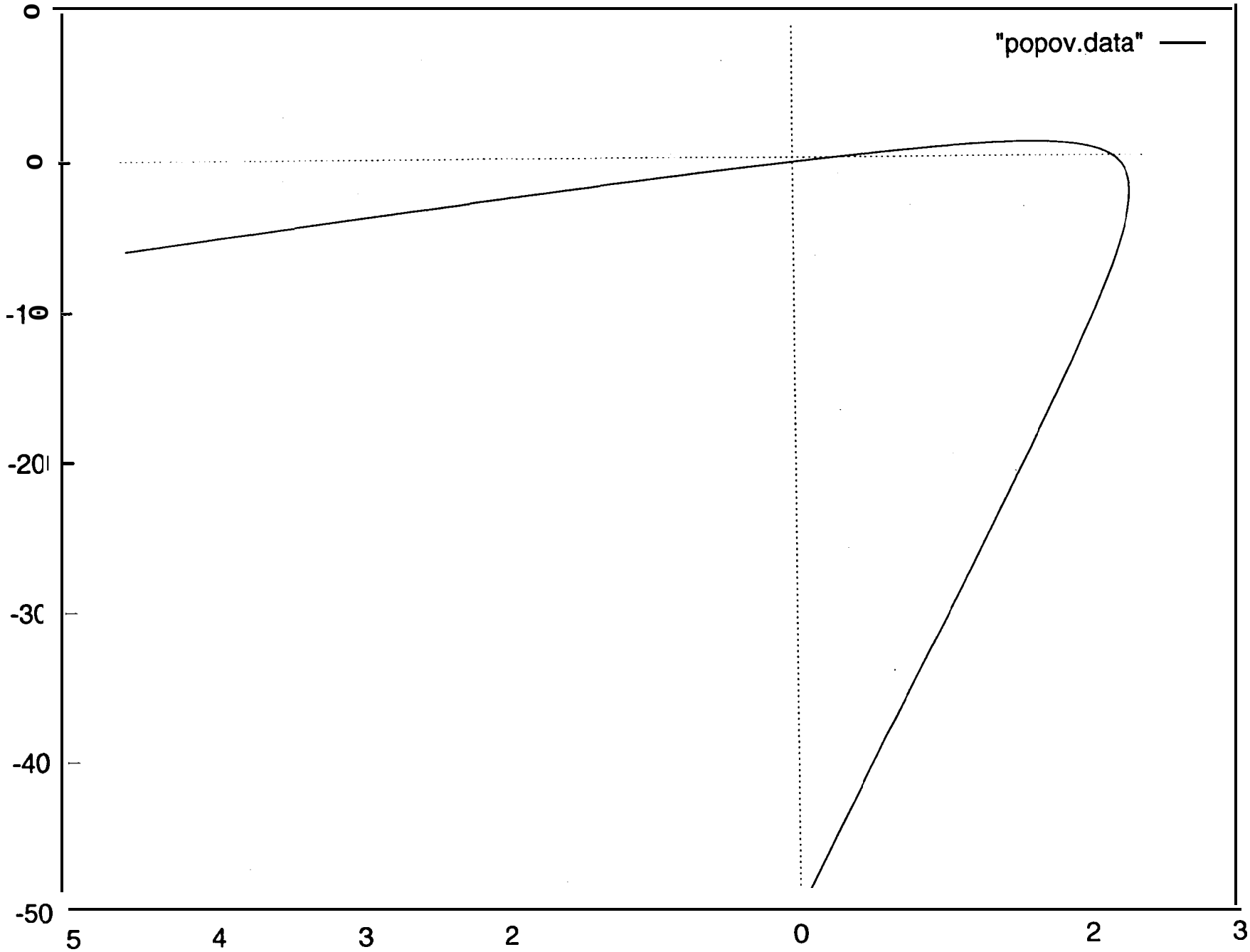

Figure 8b: Popov plot for the nonlinear PID-controlled system with $k_d = 2$